

## Evidence for ion transport and molecular ion dominance in the Venus ionotail

D. S. Intriligator,<sup>1</sup> L. H. Brace,<sup>2</sup> P. A. Cloutier,<sup>3</sup> J. M. Grebowsky,<sup>4</sup> R. E. Hartle,<sup>4</sup> W. T. Kasprzak,<sup>4</sup> W. C. Knudsen,<sup>5</sup> and R. J. Strangeway<sup>6</sup>

**Abstract.** We present analyses from the five Pioneer Venus Orbiter plasma experiments and the plasma wave experiment when a patch of plasma with enhanced densities was encountered in the near-Venus ionotail during atmospheric entry at an altitude of  $\sim 1100$  km in the nightside ionosphere. Our analyses of the thermal and superthermal ion measurements in this plasma feature provides the first evidence that at times molecular ions in the 28–32 amu mass range are dominant over atomic mass species thus yielding evidence for a transport mechanism that reaches into the lower ionosphere. Analysis of plasma analyzer (OPA) observations at this time indicates the presence of ions measured in the rest frame of the spacecraft at  $\sim 27$  and 37 volt energy per unit charge steps. In the rest frame of the planet these superthermal ions are flowing from the dawn direction at speeds (assuming they are  $O^+$ ) of  $\sim 8$  km/s and with a flow component downward (perpendicular to the ecliptic plane) at speeds of  $\sim 2$  km/s. OPA analyses also determine the ion number flux, energy, flow angles, and angular distributions. Plasma wave bursts appear to indicate that plasma density decreases within and on the equatorward edge of the patch of enhanced plasma densities are associated with ion acoustic waves and relative ion streaming.

### Introduction

We present analyses of a plasma feature observed during atmospheric entry in the nightside Venus ionosphere. While we observe the feature for the first time, in fact it may be quite common, but the instrument configurations and orbiter location were rarely optimal for its detection. During our event all five of the Pioneer Venus Orbiter (PVO) plasma instruments were appropriately configured and 27 and 37 V ion flux enhancements were present in the orbiter plasma analyzer (OPA) data. We analyze these OPA measurements obtained in the low-energy (0 to +250 V) ion mode [Intriligator *et al.*, 1980]. We also analyze simultaneous orbiter electron temperature probe (OETP)

Langmuir probe observations [Brace *et al.*, 1980]; orbiter ion mass spectrometer measurements (OIMS) [Taylor *et al.*, 1980]; orbiter retarding potential analyzer (ORPA) results [Knudsen *et al.*, 1980]; orbiter neutral mass spectrometer (ONMS) observations [Niemann *et al.*, 1980]; and OEPD orbiter electric field data [Scarfe *et al.*, 1980] measurements.

This is the first publication of analyses of the OPA plasma measurements during atmospheric entry in the near ( $< 1 R_p$ ) Venus ionotail. Vaisberg *et al.* [1977] discussed Venera 9 and 10 measurements in this region. Brace *et al.* [1987] described the ionotail of Venus as the near-tail region where the ionosphere becomes increasingly filamentary with increasing altitude, apparently forming cometlike tail rays that extend several thousand kilometers behind the planet.

### Analysis of Measurements

Figure 1a shows the OPA low-energy ion plasma flux as a function of time during the nightside periapsis passage on orbit 4574 on June 14, 1991. Except for the ionosheath fluxes at the end of this time interval ( $> 4800$  s), the highest OPA fluxes are observed from 3911 to 3963 s which we will refer to as the  $\sim 3900$  s plasma feature in the nightside ionosphere. The trajectory information at the bottom of Figure 1 indicates that this superthermal ion feature was traversed at an altitude of  $\sim 1100$  km, a latitude of  $+12^\circ$ , a longitude of  $+103^\circ$ , a solar zenith angle of  $165^\circ$ , and at a local time of 0.6 hour. The OETP electron densities are shown in Figure 1b. The dark vertical bars along the bottom represent the region where the spacecraft was in the optical umbra of Venus and serve to illustrate the scale size of the ionotail structures relative to the size of the planet.

<sup>1</sup>Space Plasma Laboratory, Carmel Research Center, Santa Monica, California.

<sup>2</sup>Space Research Laboratory, University of Michigan, Ann Arbor, Michigan.

<sup>3</sup>Space Physics Department, Rice University, Houston, Texas.

<sup>4</sup>NASA Goddard Space Flight Center, Greenbelt, Maryland.

<sup>5</sup>Knudsen Geophysical Research, Monte Sereno, California.

<sup>6</sup>Institute of Geophysics and Planetary Physics, University of California, Los Angeles.

Copyright 1994 by the American Geophysical Union.

Paper number 94JA01341.

0148-0227/94/94JA-01341\$05.00

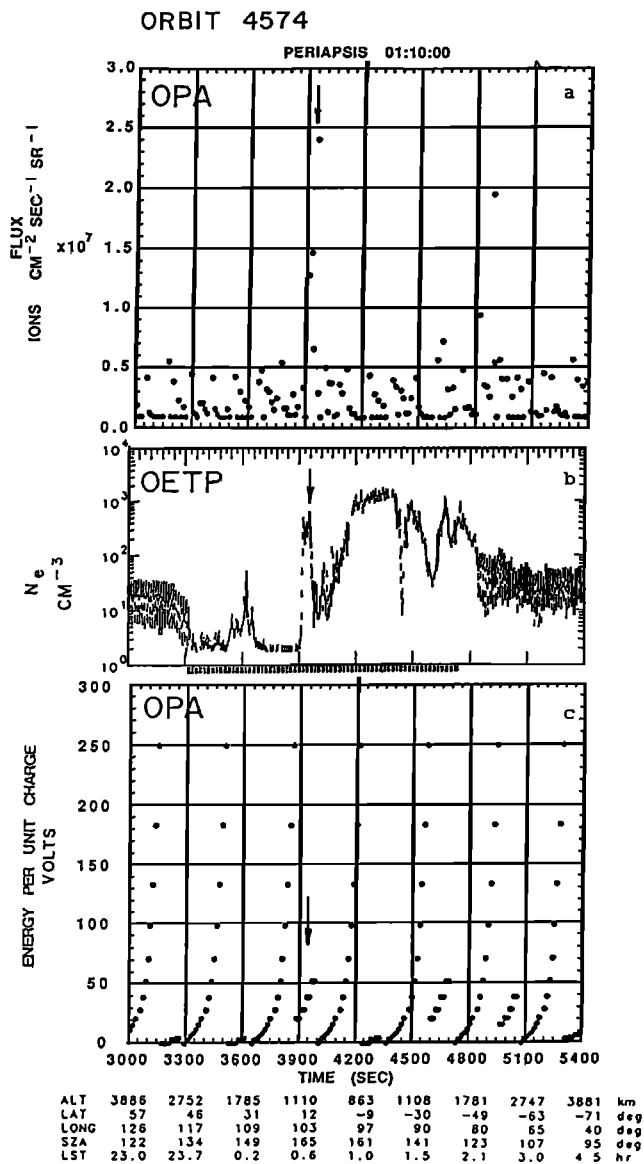


**Figure 1.** (a) Orbiter plasma analyzer (OPA) low energy ion plasma flux (using measurements obtained  $\sim 13$  s apart) as a function of time during nightside periapsis on orbit 4574 on June 14, 1992. The highest fluxes are associated with a superthermal ion feature near 3900 s. (b) Orbiter electron temperature probe (OETP) electron densities as a function time on orbit 4574. The superthermal ion feature at  $\sim 3900$  s is evident in these data. (c) OPA low-energy ion energy per unit charge ( $E/Q$ ) steps (obtained  $\sim 13$  s apart) in volts as a function of time. Each 16  $E/Q$  step maximum flux scan is followed by a 4  $E/Q$  step angular scan in the vicinity of the  $E/Q$  step where the peak flux was measured during the previous 16  $E/Q$  step maximum flux scan [Intriligator *et al.*, 1980]. As Pioneer Venus Orbiter (PVO) traversed the  $\sim 3900$  s plasma features the OPA coincidentally was performing angular scans at 27 and 37 V.

In this panel the plasma feature at  $\sim 3900$  s is evident, as is its limited spatial and/or temporal extent. Since the feature is so narrow, only a small portion of the OPAs energy and angular scans coincide with the spacecraft's

traversal of the feature. Inspection of Figure 1c indicates that these 27 and 37 V measurements were made in the four  $E/Q$  step polar and azimuthal angular scans following the sixteen  $E/Q$  step maximum flux scan [Intriligator *et al.* 1980]. Comparison of Figures 1a, 1b, and 1c indicates that it was simply coincidental that the OPA energy cycle was at the 27 and 37 V  $E/Q$  steps in the vicinity of the plasma feature. Thus, from the OPA measurements alone it is only possible to conclude that 27 and 37 V ions in the rest frame of the spacecraft were present in association with the plasma feature, and it is not possible to conclude whether lower-energy or higher-energy ions also were present. Thus it is not possible to obtain agreement with the total density measurements from other instruments.

In Figure 2 we show a schematic of the location of the plasma feature and the southward motion of the spacecraft. The OPA orientation and the field of view also are shown and these will be discussed later.

Figure 3a shows the densities from the OIMS, OETP, OPA, and ORPA, and also the OPA flux as a function of time. The plasma feature  $\sim 3900$  s that we are focusing on is evident in all these data sets between  $\sim 3900$  and 3960 s. The OIMS densities show a small rise in the  $0^+$  density (the open circles) and very large increases in the  $0_2^+$  density (the crosses) and in the  $N0^+$  density (the open squares). Mass 28 ions also were present with densities comparable to those of  $0_2^+$ . It is clear from the OIMS observations that primarily thermal molecular ions in the 28–32 amu mass range are dominant over thermal atomic ion species. It is likely that crosstalk [e.g., Grebowsky *et al.*, 1993] between signals for the 32 amu ions and the signals in nearby mass channels (e.g., those for 30 and 28 amu ions) produce current signals in the 28 and 30 amu settings that add to the current collection of ambient ions with the same masses. When we use the term crosstalk for the OIMS response, it must be emphasized that this does not mean that only a fraction of the source ion species current that should be collected at the proper amu setting is spilling into an anomalous mass setting. As discussed by Grebowsky *et al.*, [1993], superthermal ions or offsets in internal OIMS voltages from nominal operating conditions, can produce a detuning of the response of the instrument. In such a case the current collected at an anomalous mass setting can exceed the current measured at the correct setting for an incoming ion species. An analysis of the instrument response for example indicates this to be the case for 28 amu signatures that are produced by superthermal 30 or 32 amu ions. Hence one cannot use the OIMS deduced molecular ion concentrations in this obviously perturbed region of space to infer unambiguously the dominant molecular ion species, but it is certain that thermal molecular ions in the 28–32 amu mass range are dominant and that  $0^+$  is a minor constituent. For example, it is evident in Figure 3a that the measured  $0^+$  densities (as well as  $H^+$  which is not plotted) are far lower than the total electron density measured in the OETP. The computed molecular densities, on the other hand, are comparable to the electron densities (the dark circles).

To further examine the ion composition associated with

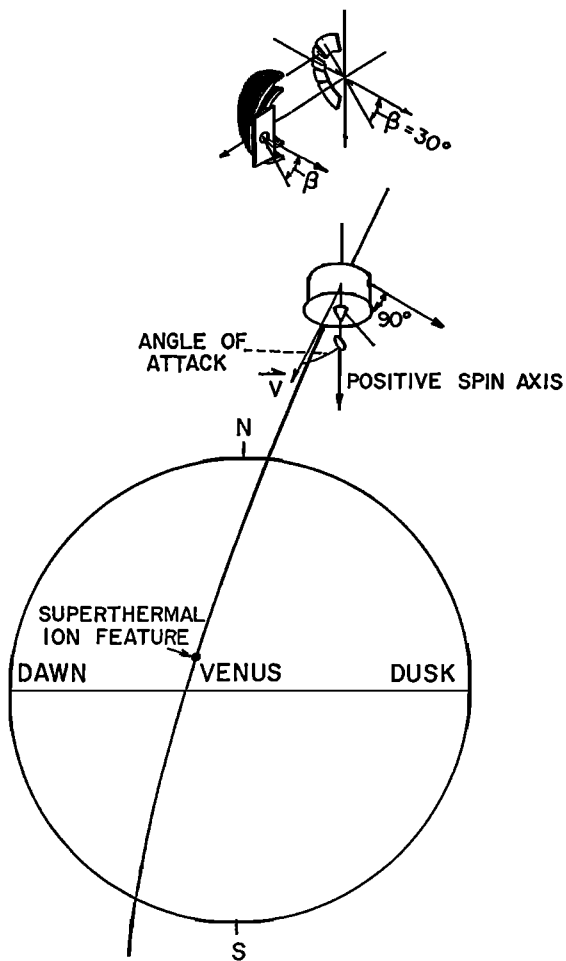


**Figure 2.** Schematic illustration of PVO angle of attack and orientation and the location of the plasma feature. The OPA field of view, circular entrance aperture, curved plates, and the array of five current collectors beyond the exit aperture are also shown. The OPA simulations show that in the spacecraft frame the  $\beta$  angle is  $30^\circ$  northward flow (with respect to the ecliptic plane) associated with the plasma feature. However, in the rest frame of the planet, since the spacecraft is mainly moving south at this time, the OPA measurements indicate a southward component of flow (see text). The superthermal ion feature  $\sim 3900$  s is primarily associated with OPA azimuthal flow  $\sim -90^\circ$  which is flow from the dawn direction.

the region under consideration,  $0\frac{1}{2}$  (mass 32) and  $0^+$  (mass 16) for energies  $>36$  eV measurements of the ONMS fluxes are shown in Figure 3b as a function of time. These measurements clearly show that there is a substantial peak in the  $0\frac{1}{2}$  superthermal fluxes (the open squares) in association with the plasma feature at  $\sim 3900$  s. The ONMS also sees enhanced superthermal 30 amu ions. Hence it is assumed that molecular superthermal ions are part of the bulk distribution. The ONMS measurements above 36 eV clearly provide more evidence that molecular ions (e.g.,  $0\frac{1}{2}$ ) and not atomic ions (e.g.,  $0^+$ ) are dominant within the patch of enhanced plasma fluxes. Comparison of the magnitudes of the superthermal  $0\frac{1}{2}$

fluxes relative to the  $0^+$  fluxes from the ONMS (Figure 3b) with the corresponding ratios of ion densities deduced by the OIMS (Figure 3a) for the same masses indicate that in both energy regimes the molecular ion abundances are more than an order of magnitude above those of the  $0^+$  in the plasma feature.

At this time the ORPA also measures increased ion densities and the OPA measures increased ion fluxes, but these instruments by themselves cannot unambiguously determine the ion masses. On the basis of OIMS and ONMS determinations, we assume that  $0\frac{1}{2}$  is the most abundant species, and this is accepted for interpretation of the ORPA measurements and the OPA simulation. The ORPA results and the results of the OPA simulations (see below) are relatively insensitive to whether mass 28, 30, or 32 is assumed. We derive a thermal  $0\frac{1}{2}$  density of  $373\text{ cm}^{-3}$

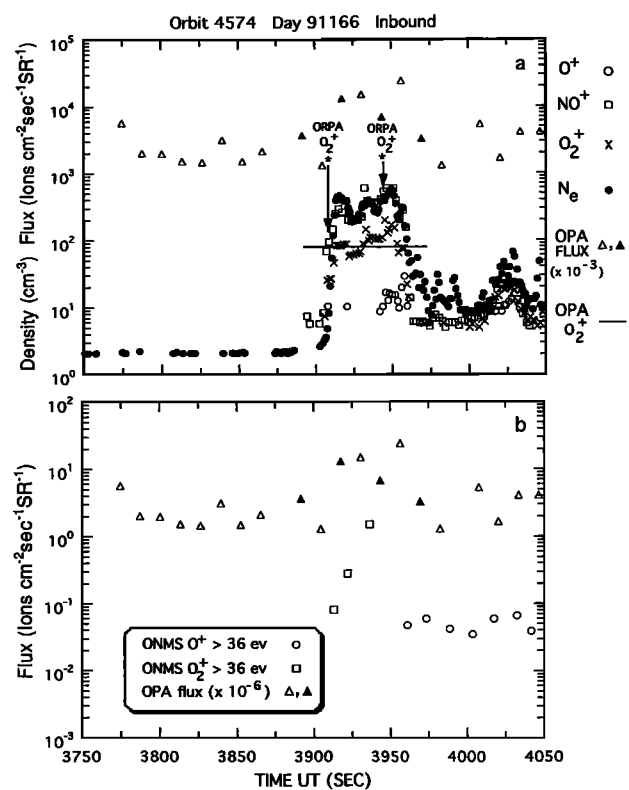


**Figure 3.** (a) Orbiter ion mass spectrometer (OIMS), OETP, orbiter retarding potential analyzer (ORPA), and OPA densities and OPA flux as a function of time in the vicinity of the plasma feature. The tip of the arrow indicates the actual location of the ORPA densities. The OIMS measurements show molecular ions are dominant (see text). The solid triangles indicate the OPA polar scan fluxes used as input in the simulation (see Figure 5). The straight line shows the OPA density estimated in the simulation. The narrow temporal/spatial extent of the plasma feature introduces uncertainties in the OPA density estimates. The OPA estimate could be lower than the ambient density but the magnitude of the uncertainties is difficult to assess (see text). (b) Orbiter neutral mass spectrometer (ONMS) and OPA fluxes as a function of time. Note that the ONMS identifies  $0\frac{1}{2}$  as the dominant ion in this plasma feature.

from the ORPA observations at 3942 s, a number that is consistent with the  $N_e$  measurements. This is derived based on the measurements in a 0.16 s I-V scan using the ORPA measured vehicle potential of -0.6 V and the knowledge of the exact orientation of the ORPA axis with respect to the spacecraft velocity vector at the time of measurement. Similarly, at 3909 s, on the polarward edge of the feature, the ORPA density is  $124 \text{ cm}^{-3}$  for thermal  $0\frac{1}{2}$ .  $0\frac{1}{2}$  temperatures and velocities were also derived and these will be discussed in the relevant sections below. The ORPA densities are denoted by the end of the arrows from the asterisks in Figure 3a.

The  $0\frac{1}{2}$  density for the higher energy population estimated from the OPA simulations (see Figure 4) is  $\sim 80 \text{ cm}^{-3}$  and is denoted by the horizontal line in Figure 3a. The input data (the solid triangles in Figure 3) used in the OPA instrument simulation were the ion fluxes obtained on collectors 5 and 4 in the polar scan on four  $E/Q$  steps in the vicinity of the peak [Intriligator *et al.*, 1980]. These observations were obtained between 3891.5 and 3969.5 s. We emphasize the narrow time/spatial extent of the plasma event. The OPA observations contain contributions from spatial and/or temporal variations whose magnitude cannot be easily assessed. This may result in our obtaining a lower density and a lower temperature than those characteristic of the ambient plasma since, for the purpose of this simulation we assumed a quasi-steady state during this 78 s time interval. As emphasized by the four solid triangles in Figure 3, this does not appear to be the case, but it allows us to fit the four solid triangles with one distribution function. A convecting Maxwell-Boltzmann plasma distribution function was assumed. The output of the simulation is the plasma parameters - density, temperature, speed, and north-south angles of flow associated with the distribution. The east-west (azimuthal) flow angle distributions in the ecliptic plane are determined independently in the azimuthal scans and are shown in Figure 5. Since the duration of the plasma feature only extended from  $\sim 3910$  to 3950 s, only

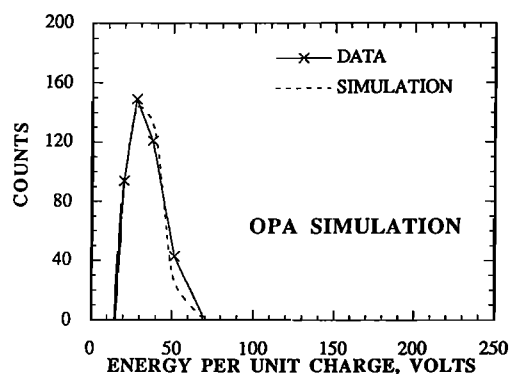


**Figure 4.** OPA low-energy ion flux (solid line) obtained on collector 5 in the polar scan as a function of volts for the four  $E/Q$  steps, that is, the solid triangles in Figure 3 in the vicinity of the plasma feature. Results of a preliminary instrument simulation of these 78 s of data are indicated by the dashed line. The assumptions and uncertainties associated with the simulation are discussed in the text.

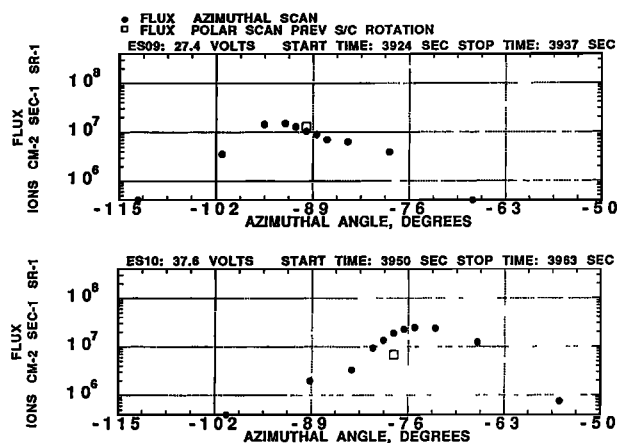


**Figure 5.** OPA azimuthal angle distributions showing the flux as a function of azimuthal angle for the 27 V (upper) and 37 V (lower)  $E/Q$  steps. The peak polar angle at each energy step is obtained  $\sim 13$  s (i.e., one spacecraft revolution) before the peak azimuthal angle for that energy step. The duration of each of the data points is  $\sim 25$  ms. The angular scans shown here were obtained in four sequential spacecraft rotations (polar 27 V, azimuthal 27 V, polar 37 V, azimuthal 37 V). The negative angles denote flow from the east. The 27 V scan peaks at  $\sim -89^\circ$  indicating that these ions are flowing from the east horizontally (parallel to the surface of Venus) which means that the flow in this poleward portion of the plasma feature is from the dawn direction. The 37 V azimuthal scan peaks at  $\sim -77^\circ$  indicating a slight component of the flow directed outward from the planet at the equatorward edge of the feature.

one set of polar scans was obtained near it (and these straddle the feature as shown in Figure 3), and, thus only one set of parameters could be obtained from the simulation. These simulations also indicated that in the spacecraft frame the polar flow is  $\sim 30^\circ$  from the ecliptic plane to the north, i.e., flow from the south (see below). In the rest frame of the planet the flow has a component to the south. The  $0\frac{1}{2}$  temperature and speed estimates are discussed below.

It should be noted that the OETP measures the electron (i.e., total ion) density. The ORPA, OIMS, ONMS measurements, and to some extent the OPA measurements, are dependent on the flow characteristics of the ions with respect to the instrument apertures.

With respect to plasma temperatures the OETP measurements yield an electron temperature of  $\sim 7000\text{K}$ , which is typical of the nightside ionosphere at this altitude. The ORPA derivation at 3942 s in the plasma feature yields an  $0\frac{1}{2}$  temperature of 10,237K and at 3904 s a temperature of 17,394K is obtained on the poleward edge of the feature. In the plasma feature the OPA simulation estimates a temperature of  $\sim 10,000 \pm 250\text{K}$  which, as discussed above, may be lower than the ambient plasma temperature since measurements were only obtained on two energy steps in the plasma feature due to its limited spatial/temporal extent.

The component of the ORPA ion bulk velocity parallel to the instrument axis was calculated. It is positive when directed along the outward direction of the instrument axis. At 3942 s in the plasma feature the direction cosines of the ORPA instrument axis in solar ecliptic coordinates were 0.35, -0.2, and -0.94. At 3942 s the velocity component along the instrument axis derived from the 0.16 s sweep was +0.46 km/s. Similarly, at 3909 s on the poleward edge of the plasma feature, the comparable direction cosines of the ORPA axis were -0.48, 0.12, and -0.87 and the component of velocity along the ORPA instrument axis was +1.93 km/s. The OPA simulation shown in Figure 4 yields an  $0\frac{1}{2}$  bulk speed in the spacecraft frame of  $\sim 12.5$  km/s after correcting for vehicle potential.

It is useful to convert the OPA velocity from the rest frame of the spacecraft to the planet's rest frame. The OPA measures (see Figures 2 and 5) the peak azimuthal flow direction as  $\sim -90^\circ$  (for the 27.4 V polar and azimuthal scans). If we assume that  $-90^\circ$ , flow from dawn to dusk, is the azimuthal flow direction ( $\phi$ ) and as determined from the OPA simulation  $\beta = 30^\circ$  (Figure 2) is the north-south flow direction then we obtain (0, -10.8, +6.3) for the relative ion velocity in solar ecliptic coordinates with respect to the spacecraft. Using the 3942 s values for the spacecraft velocity (+0.19, +2.51, -8.77), then we obtain (+0.19, -8.3, -2.5) for the ion velocity relative to the planet. This implies that the ions measured by the OPA are predominantly moving toward the negative Y component (i.e., to dusk from dawn) at 8.3 km/s and downward (toward the south with respect to the ecliptic plane) at 2.5 km/s. (If there had been no Z (north-south) component of flow then the OPA should have been 8.77 instead of 6.3 as the Z component.)

To compare the OPA velocity (derived by combining and then fitting samples obtained between 3911 and 3950 s) with the ORPA velocity component along the direction of the ORPA instrument axis (derived from a 0.16 s sample at 3942 s) we dot the OPA velocity vector into the direction of the ORPA instrument axis. This yields +4.1 km/s but the ORPA measures +0.46 km/s at 3942 s. This discrepancy may be due to changes in the flow parameters in the plasma feature since the OPA simulation assumes a steady state from the first polar scan peak flux to the fourth polar scan peak flux ( $\sim 3892$  s to 3970 s). However, the OPA azimuthal angle scans (Figure 5) indicate a  $12^\circ$  change in azimuthal flow during this time and the density profiles (Figures 3a and 3b) also show changes during this time.

In order to clearly focus on the azimuthal flow angles, Figure 5 shows angular distributions. These azimuthal scans look very real with a well-defined direction. They indicate flow from dawn to dusk in agreement with the ONMS results which represent ions with energies exceeding 36 V (see Figure 6 and text below).

Figure 6 shows the azimuthal flow angles of the superthermal component of the ions measured by the ONMS. The  $0\frac{1}{2}$  flow angle in association with the plasma feature between  $\sim 3910$  and 3960 s is  $\sim -80^\circ$  to  $-110^\circ$ . In the ONMS convention this represents flow from the dawn

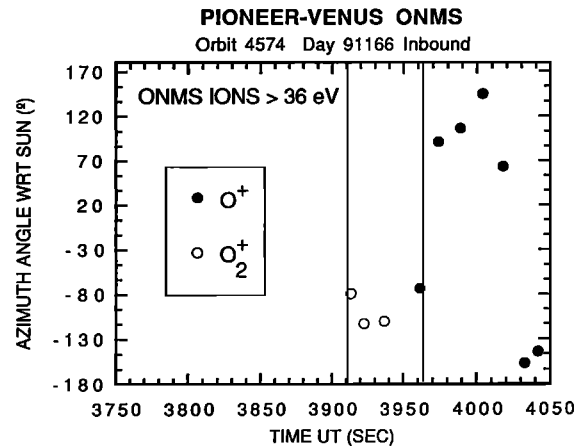


**Figure 6.** ONMS azimuthal flow angle as a function of time on the same time scale as in Figure 3. The  $0\frac{1}{2}$  flows between  $\sim 3910$  and 3960 s are in the vicinity of  $\sim 80^\circ$  to  $-110^\circ$ . These  $0\frac{1}{2}$  flow angles indicate dawn to dusk flow and are consistent with the  $0\frac{1}{2}$  flow angles from the OPA (Figure 5).

direction. Thus the ONMS and the OPA azimuthal flow information agree.

In Figure 7 we present the high-resolution OEFD plasma wave observations for the 100-Hz, 730-Hz, 5.4-kHz, and 30-kHz channels for the same time interval as that shown in Figures 3a, 3b, and 6. There are enhancements in the plasma wave signals in the 730-Hz and 5.4-kHz channels associated with the plasma feature at  $\sim 3900$  s. There is a step-like rise, particularly in the 5.4-kHz channel and to a lesser extent in the 730-Hz channel between  $\sim 3910$  and 3960 s that clearly corresponds to the increase in plasma density associated with the  $\sim 3900$  s plasma feature as seen in the OETP data and in the other plasma observations in Figure 3. Between  $\sim 3920$  and 3930 s there is a large plasma wave burst which is particularly evident in the 730-Hz channel and to a lesser extent in the 5.4-kHz channel. Comparison of the plasma data in Figure 3 with this plasma wave burst indicates that the burst is coincident with the decrease in plasma density in the OETP and OIMS data. This 730-Hz and 5.4-kHz burst may be indicative of the presence of ion acoustic waves. These waves could be the result of flows in the plasma similar to the ion streaming near the magnetotail boundary in the extended Venus tail region where ion acoustic waves were present [Intriligator and Scarf, 1984]. For example, there could be relative streaming between two ion species (e.g.,  $0\frac{1}{2}$  and  $0^+$ ) or relative streaming between ions of the same species where the ions in one of the streams have been accelerated at some other location. There is another set of 730-Hz and 5.4-kHz bursts which occurs between 3950 and 3960 s. Again, comparing the timing of this set of bursts with the plasma data in Figure 3 indicates that these bursts are coincident with the first sharp density decrease at the equatorward edge of the plasma feature. Similarly, the smaller plasma wave spikes in the 730-Hz channel (and less discernably but still present in the 5.4-kHz channel)

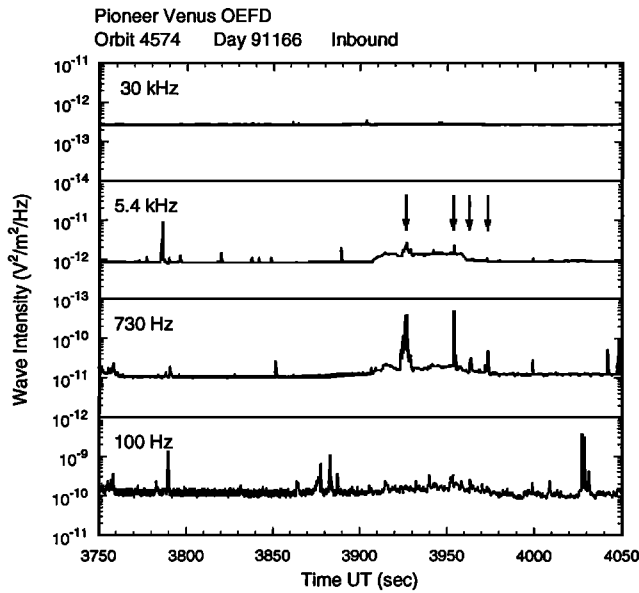


**Figure 7.** OEFD plasma wave signals in four channels as a function of time on the same time scale as in Figure 3. Enhanced signals are evident (e.g., between 3920 and 3930 s, between 3950 and 3960 s) in the 730-Hz and 5.4-kHz channels, in association with sharp density decreases within the superthermal ion feature and along its equatorward edge. The arrows denote regions associated with simultaneous plasma density decreases (see Figure 3).

between 3960 and 3970 s and again between 3970 and 3980 s also correspond to steplike decreases in the OETP plasma density (see Figure 3). All of the plasma wave enhancements are most likely associated with ion acoustic waves due to relative ion streaming in the plasma. The behavior of the magnetic field data at the time of the plasma feature ( $\sim 3900$  s) is difficult to resolve (since the only component available is perpendicular to the ecliptic plane and it exhibits an offset that may not be physical [C. T. Russell, private communication, 1993], but there does appear to be a small increase in  $B_z$  (the component perpendicular to the ecliptic plane) just before the plasma feature.

## Discussion

We have chosen a specific plasma feature to study since modes of all five of the PVO plasma instruments were appropriately configured at this time and low-energy ion flux enhancements were present in the OPA data. These circumstances occur rarely or can only rarely be seen because of instrument cycling. All five of the PVO plasma measurements indicate a spikelike spatial and/or temporal gradient is associated with this plasma feature. The OIMS and the ONMS measurements indicate that it is primarily associated with molecular ions (e.g.,  $O_2^+$ ) and not atomic ions (e.g.,  $O^+$ ). The OETP, OIMS, and ORPA measurements indicate that the total ion densities are of the order of  $300\text{--}500\text{ cm}^{-3}$ . The OPA simulation estimates superthermal molecular densities on the order of  $\sim 80\text{ cm}^{-3}$ . This

estimate may be lower than the ambient density due to the narrowness of the plasma feature as discussed above.

As a result of the present study, we are able to make an independent determination of the superthermal plasma fluxes, of their energies, and the angles of flow both in the ecliptic plane and perpendicular to it. We also are able to determine that primarily molecular ions (e.g.,  $O_2^+$ ) are present and that the instruments appear to be sampling different regimes of the same energy distribution function. We also conclude that ion transport is taking place and that the velocity changes in magnitude and direction across the feature. The plasma wave observations indicate that, within the feature and along the equatorward edge of the feature, ion acoustic waves are present that may be indicative of relative ion streaming. These waves appear to occur when there are sharp density decreases in the plasma. The dominance of molecular ions (e.g., in the ONMS measurements) suggests that the ions originate from altitudes below 200 km which is the only region where chemical processes exist which can produce molecular ions at concentrations exceeding those of the atomic ions.

*Kar et al.*, [1994] have recently shown that day-to-night transport of ionospheric plasma was diminished considerably near solar minimum. Consequently, it is not too likely that the  $O_2^+$  produced on the dayside was flowing to the nightside during the time when  $O_2^+$  was observed in the ionotail. The dominance of  $O_2^+$  in the ionotail is, however, consistent with the nightside ionospheric plasma being transported upward from the  $O_2^+$  peak region. The recent reentry OIMS measurements of the nightside ionosphere near solar minimum revealed that  $O_2^+$  was at least an order of magnitude more dense than  $O^+$  at the ionization peak; furthermore, analysis of this ionization layer showed that it was produced primarily by electron impact ionization [Kar et al., 1994]. Thus it is quite natural to expect ions to tend to fill a "void" and flow away from their source region and, at least occasionally, be accelerated to the high energies observed. Such a scenario leads to  $O_2^+$  being the dominant ion in the ionotail, with  $O^+$  flowing upward with a proportionately lower concentration level (too low to be observed by the OIMS and near background count rates by the ONMS). The horizontal component of the observed flow would seem to indicate that the acceleration could be occurring near the terminator.

The PVO observations are consistent with this scenario. The ONMS and OPA azimuthal flow angles ( $\sim -90^\circ$ ) indicate flow into the instruments from the dawn direction and at times (equatorward of the feature when the flow is  $-77^\circ$ ) with some component outward from the planet. The OPA polar (north-south) flow information indicates that the flow is directed northward at an angle of  $\sim 30^\circ$  to the ecliptic plane (i.e., it originates in the south). This polar flow direction is consistent with the ram direction of the spacecraft at this time as the spacecraft is traveling from the north to the south (see Figure 2). The OPA simulation, after correcting for the spacecraft velocity and vehicle potential, provides a total  $O_2^+$  drift speed of  $\sim 8.7\text{ km/s}$  which does not exceed the escape speed ( $\sim 10\text{ km/s}$ ). It is possible that the OPA speed is lower than the ambient  $O_2^+$

speed if the limited extent of the event precluded obtaining accurate data within the plasma feature. The enhanced plasma wave activities associated with the plasma feature are consistent with the presence of relative ion streaming. Perhaps the plasma wave bursts are indicative of the upward flow or the acceleration of molecular ions. The OETP electron temperature of 7000K and the ORPA (at 3942 s) and OPA (based on 3891.5 to 3969.5 s data) temperatures of  $\sim 10,000$ K are consistent with an ionospheric source for the plasma feature assuming that all instruments are sampling parts of the same  $O_2^+$  energy distribution function. However, due to the narrowness of the plasma feature the OPA temperature estimate may be low since measurements only were made on two energy steps in the plasma feature.

*Brace et al.* [1987] discussed the uncertainty in determining the magnitude of the superthermal ion energy based solely on the OIMS measurements. The OPA measurements presented here provide evidence for ions with energy per unit charge of 27 and 37 V in the rest frame of the spacecraft. On the basis of comparisons with the ONMS and OIMS we conclude these are primarily  $O_2^+$  ions.

We have presented the first analysis of OPA low-energy ion measurements during atmospheric entry in the nightside Venus ionosphere. We provided the first plasma density, speed, components of flow, and temperature analysis for the low energy ion OPA measurements. We obtain OPA measurements at 27 and 37 V, the plasma number flux, and angles of flow. We present (Figure 5) the first azimuthal angular distributions of OPA measurements. These parameters are generally consistent with those from the other plasma instruments. This is also the case for the plasma parameters derived from the ORPA observations obtained in two different 0.16 s sweeps. However, the OPA velocity dotted into the ORPA instrument axis yields a different (larger) velocity component than that measured by the ORPA. Since the OPA determination assumes steady state and we know that between 3911 and 3950 s conditions are changing this could be why the ORPA value at 3942 s is different.

There is general agreement between the superthermal fluxes as measured by the ONMS and the OPA. *Kasprzak et al.* [1991] report that the average  $O^+$  flux for  $O^+$  ions  $> 36$  eV measured by the ONMS is about  $10^5 \text{ cm}^{-2} \text{ s}^{-1}$  but that higher fluxes from  $10^6$  to  $10^8 \text{ cm}^{-2} \text{ s}^{-1}$  have been observed about 10% of the time.  $O^+$  fluxes on the order of  $\sim 10^5$  are observed by the ONMS in association with the superthermal plasma feature. The peak  $O_2^+$  fluxes above 36 V measured by the ONMS in the superthermal plasma feature sharply increase over an order of magnitude to reach  $\sim 5 \times 10^6$ . The low-energy ion fluxes measured by the OPA in the plasma feature also show a sharp increase with a maximum flux near  $2 \times 10^7$ . If it is assumed that the ONMS is measuring that portion of the OPA distribution shown in Figure 6 above 36 eV then approximately 20% of the ion flux observed by the OPA is being measured by the ONMS. This assumes an ONMS transmission with energy based on laboratory data [*Kasprzak et al.*, 1987]. A similar ratio of about 25% is observed in the maximum flux ratio.

These results are consistent with the ONMS measuring the high-energy tail of a plasma distribution with a lower mean energy as determined by the OPA.

*Brace et al.* [1987] found a weakened magnetic field in the rays and that a strong steady tailward magnetic field dominates the trough regions surrounding the rays. They also found that an approximate pressure balance existed across ray boundaries, with the static plasma pressure of the rays balanced by the magnetic pressure of the surrounding trough regions. From the available  $B_z$  magnetic field data on orbit 4574,  $B_z$  appears to peak just before the plasma feature; however, no reliable magnetic field data are available in the feature.

The specific plasma feature we examined is a patch of enhanced plasma densities. It could be associated with a tail ray.

## Conclusions

In this paper we conclude the following:

1. A plasma event occurred in the nightside Venus ionosphere on June 14, 1992. The event occurs rarely or only rarely can be seen if it is quite common since instrument configurations and orbiter location were rarely optimal for its detection.
2. The apparent duration of the event was  $\sim 1$  min.
3. The event was measured by all five PVO plasma experiments (OETP, OIMS, ONMS, ORPA, and OPA) and the plasma wave experiment (OEPD).
4. The event was associated with a patch of plasma with enhanced thermal and superthermal densities.
5. For thermals the OIMS determined that molecular ions in the 28-32 amu mass range were dominant over atomic ion species.
6. For superthermal ( $> 36$  eV) the ONMS found that molecular ions (i.e.,  $O_2^+$ ) were dominant over atomic ions.
7. The molecular ion dominance is suggestive of a source in the deep ionosphere.
8. The molecular ions are flowing from the dawn direction as determined by both the ONMS and OPA.
9. The total ion densities are  $\sim 300\text{-}500 \text{ cm}^{-3}$  based on the OETP, OIMS, and ORPA results.
10. Electron temperatures of 7000K were found by the OETP.
11. Thermal ion temperatures of  $\sim 10,000$ K were obtained by the ORPA and OPA but the OPA temperature may be low.
12. The temperature measurements are also consistent with an ionospheric source for the feature.
13. The OPA density and temperature estimates may be lower than the ambient values due to the narrowness of the plasma feature.
14. There is general agreement between the superthermal fluxes as measured by the ONMS and the OPA.
15. Plasma wave bursts within and on the equatorward edge of the event appear to be associated with ion acoustic waves and relative ion streaming.

**Acknowledgments.** We are indebted to the Pioneer Project Office for the success of PVO. This work was supported in part by NASA Ames Research Center under contract NAS2-12912, by NASA Headquarters Venus Data Analysis Program under contract NASW-4815, and by Carmel Research Center. We are grateful to C. T. Russell for providing the magnetometer data. Hanchen Huang ran the OPA simulations after David Miller modified the simulation program developed by Ken Intriligator and James Intriligator. We thank D. Hunten and two referees for constructive comments.

The Editor thanks three referees for their assistance in evaluating this paper.

## References

- Brace, L. H., R. F. Theis, W. R. Hoegy, J. H. Wolfe, J. D. Mihalov, C. T. Russell, E. C. Elphic, and A. F. Nagy, The dynamic behavior of the Venus ionosphere in response to solar wind interactions, *J. Geophys. Res.*, **85**, 7663, 1980.
- Brace, L. H., W. T. Kasprzak, H. A. Taylor, R. F. Theis, C. T. Russell, A. Barnes, J. D. Mihalov, and D. M. Hunten, The ionotail of Venus: Its configuration and evidence for ion escape, *J. Geophys. Res.*, **92**, 15, 1987.
- Grebowsky, J. M., W. T. Kasprzak, R. E. Hartle, K. K. Mahajan, and T. C. G. Wagner, Superthermal ions detected in Venus' dayside ionosheath, ionopause and magnetic barrier regions, *J. Geophys. Res.*, **98**, 9055, 1993.
- Intriligator, D. S., Observations of mass addition to the shocked solar wind of the Venusian ionosheath, *Geophys. Res. Lett.*, **9**, 727, 1982.
- Intriligator, D. S., Results of the first statistical study of PVO plasma observations in the distant Venus tail: Evidence for a hemispheric asymmetry in the pickup ionospheric ions, *Geophys. Res. Lett.*, **16**, 167, 1989.
- Intriligator, D. S., and F. L. Scarf, Wave-particle interactions in the Venus wake and tail, *J. Geophys. Res.*, **89**, 47, 1984.
- Intriligator, D. S., J. Wolfe, and J. Mihalov, The Pioneer Venus orbiter plasma analyzer experiment, *IEEE Trans. Geosci. Remote Sens.*, **GE-18**, 39, 1980.
- Kar, J., R. E. Hartle, J. M. Grebowsky, W. T. Kasprzak, T. M. Donahue, and P. A. Cloutier, Evidence of electron impact ionization on the nightside of Venus from PVO/OIMS measurements near solar minimum, *J. Geophys. Res.*, **99**, 11351, 1994.
- Kasprzak, W. T., H. A. Taylor Jr., L. H. Brace, and H. B. Niemann, Observations of energetic ions near the Venus ionopause, *Planet. Space Sci.*, **30**, 1107, 1982.
- Kasprzak, W. T., H. B. Niemann, and P. Mahaffy, Observations of energetic ions on the nightside of Venus, *J. Geophys. Res.*, **92**, 291, 1987.
- Kasprzak, W. T., J. M. Grebowsky, H. B. Neimann, and L. H. Brace, Superthermal >36-eV ions observed in the near-tail region of Venus by the Pioneer Venus Orbiter neutral mass spectrometer, *J. Geophys. Res.*, **96**, 11,175, 1991.
- Knudsen, W. C., K. L. Miller, K. Spenner, M. Novak, P. F. Michelson and R. C. Whitten, Suprathermal electron energy distribution within the dayside Venus ionosphere, *J. Geophys. Res.*, **85**, 7754, 1980.
- Mihalov, J. D., and A. Barnes, The distant interplanetary wake of Venus: Plasma observations of Pioneer Venus, *J. Geophys. Res.*, **87**, 9034, 1982.
- Niemann, H. B., J. R. Booth, J. E. Cooley, R. E. Hartle, W. T. Kasprzak, N. W. Spencer, S. H. Way, D. M. Hunten, and G. R. Carignan, Pioneer Venus orbiter neutral gas mass spectrometer, *IEEE Trans. Geosci. Remote Sens.*, **GE-18**(1), 60, 1980.
- Scarf, F. L., W. W. L. Taylor, and P. F. Virobik, The Pioneer Venus orbiter plasma wave investigation, *IEEE Trans. Geosci. Remote Sens.*, **GE-18**, 36, 1980.
- Slavin, J. A., D. S. Intriligator, and E. J. Smith, Pioneer Venus orbiter magnetic field and plasma observations in the Venus magnetotail, *J. Geophys. Res.*, **94**, 2383, 1989.
- Taylor, H. A., Jr., H. C. Brinton, S. J. Bauer, R. E. Hartle, P. A. Cloutier, and R. E. Daniell Jr., Global observations of the compression and dynamics of the ionosphere of Venus: Implications for the solar wind interaction, *J. Geophys. Res.*, **85**, 7765, 1980.
- Vaisberg, O. L., S. A. Romanov, V. N. Smirnov, I. P. Karpinskii, B. I. Khazanov, B. V. Polenov, A. V. Bogdanov, and N. M. Antonov, Structure of the region of interaction of solar wind with Venus inferred from measurement of ion-flux characteristics on Venera 9 and Venera 10, *Cosmic Res.*, **14**, 709, 1977.

---

D. S. Intriligator, Carmel Research Center, Post Office Box 1732, Santa Monica, CA 90406. (e-mail: dsintriligator@nasamail.nasa.gov)

L. H. Brace, Space Physics Research Laboratory, University of Michigan, Ann Arbor, MI 48109.

P. A. Cloutier, Space Physics, Rice University, Box 1892, Houston, TX 77251.

J. M. Grebowsky, R.E. Hartle, and W.T. Kasprzak, NASA Goddard Space Flight Center, Greenbelt, MD 20771. (e-mail: pacf::grebowsky;pacf::kasprzak)

W. C. Knudsen, Knudsen Geophysical Research, Inc., 18475 Twin Creek Rd., Monte Sereno, CA 95030.

R. J. Strangeway, IGPP, University of California, Los Angeles, Los Angeles, CA 90024. (e-mail: brunet::strangeway)

(Received June 20, 1993; revised May 13, 1994; accepted May 17, 1994.)